

## **Synthesis of PbS Functionalized With Gelatin as a Fluorescence-Enhanced Sensor for Determination of Phenylpropanolamine (PPA) Drug in Blood and Urine Samples**

Shirin Bouroumand<sup>1</sup>, Farzaneh Marahel<sup>1\*</sup> and Fereydoon Khazali<sup>2</sup>

<sup>1,2</sup> Department of Chemistry, Omidiyeh Branch, Islamic Azad University, Omidiyeh, Iran.

Received May 2020; Accepted July 2020

### **ABSTRACT**

Synthesized PbS sensor functionalized with gelatin quantum dots glutaraldehyde has been recognized as a unique medicament sensor thanks to its ultra-fine size, photo-stability, and distinguished fluorescent properties. The fluorescence of the PbS quantum dots sensor functionalized with gelatin synthesis is selectively and sensitively enhanced by addition of the Phenylpropanolamine (PPA) drug-induced aggregation of sensor PbS with gelatin. This finding was further used to design a fluorometric method for the determination of (PPA) drug. The reaction is followed fluorometrically by measuring the absorbance at 335 nm.  $2.5 \times 10^{-2}$  molL<sup>-1</sup> PbS with gelatin sensor, calibration graph in the range of 0.05 - 10.0  $\mu\text{g L}^{-1}$  (PPA) drug. The absorbance is linear from 0.05 up to 100.0  $\mu\text{g L}^{-1}$  in aqueous solution with repeatability (RSD) of 3.5% at a concentration of 10.0  $\mu\text{g L}^{-1}$  and a detection limit of 2.2  $\mu\text{g L}^{-1}$  by the fixed-time method of 60 sec. The relative standard deviation for 10.0  $\mu\text{g L}^{-1}$  (PPA) drug is %95. The applicability of the method was demonstrated by the determination of the (PPA) drug in urine and blood samples.

**Keywords:** Phenylpropanolamine (PPA) Drug; Fluorescence; Sensor PbS with Gelatin Synthesis; Quantum Dots; Determination

### **1. INTRODUCTION**

Phenylpropanolamine hydrochloride (PPA) is a nasal decongestant mainly used in combinations for relief of cold symptoms as it has indirect sympathomimetic activity [1,2]. PPA is also known as  $\beta$ -hydroxy amphetamine, and is a member of the phenethylamine and amphetamine chemical classes [3]. Pharmaceutical drug preparations of PPA have varied in their stereoisomer composition in different countries, which

may explain differences in misuse and side effect profiles [4]. Analogues of PPA include ephedrine, pseudoephedrine, amphetamine, methamphetamine, and cathinone [5]. Its chemical name is (1RS, 2SR) -2-amino -1-phenyl propanol. Te BP described non aqueous potentiometric titration for PPA [2]. Te USP suggested non-aqueous titration method using glacial acetic acid for PPA pure form and HPLC method for its capsules, extended released capsules, tablets, extended released tablets and oral solutions [6].

---

\*Corresponding author: Farzane.marahel.fm@gmail.com

In this connection, several analytical techniques such as capillary electrophoresis [7], Voltammetry [8], nanocomposites electrodes-based voltammetry [9], capillary gas chromatography HPLC [10,11,12], HPTLC [13], liquid chromatography coupled with mass spectrometry (LC-MS) [14] and spectrophotometry [15]. There are different methods used for PPA determination spectrophotometry [16] and flow injection [17]. Recently, noble metal nanoparticles-based UV-visible spectrometric and fluorometrically methods have drawn special attention for selective and sensitive reorganization of target species (inorganic, organic and biomolecules) in various complex matrices [18].

In recent years, fluorescent sensors have attracted much attention in the detection of drugs due to their excellent properties of easy operation, high sensitivity, selectivity, and real-time monitoring [19, 20]. In the past few decades, a great variety of fluorescence probes have been reported for the determination of drugs including organic dyes [21] and quantum dots (QDs) [22]. However, those QDs are limited by the potential leakage of heavy metal elements [23]. Consequently, developing alternative and environmentally friendly materials is of great significance [24]. Owing to their ultrafine size (usually less than 2 nm) [25], which is equivalent to the electronic Fermi wavelength, fluorescent sensors the nature of molecules, including discrete energy level, strong light luminescence, good light stability, biocompatibility and other unique physical

and chemical properties, thus exhibiting great potential in the field of sensing and imaging [26,27]. However, Owing to low chemical and thermal resistance as well as difficulties in separation and recovery associated with the low-molecular-weight chemosensors, a physical immobilization support is often needed for their application [28, 29]. A physical support does not only improve the mechanical properties, but also minimizes the tendency of the sensing molecules to migrate. To avoid complications associated with synthesizing probes and immobilizing them on a physical support, polymers with host binding sites as part of their backbone or as part of their pendant group were found to be better alternatives.

In the present article, an uncomplicated facile strategy was employed in preparing water-soluble, stable PbS with gelatin by utilizing glutaraldehyde as a stabilizer. As it is shown in (Fig. 1), the existence of (PPA) provokes the aggregation of nanoclusters with improvement of fluorescence intensity. In addition, successful application of nanoprobe in detecting (PPA) medicament in different real samples along with their significant efficiency and perfect recovery prove their great potentialities in practical application. In the current article, a fluorometric method was designed for determining (PPA). The extreme sensitivity, electivity and simplicity of the proposed method led to the absolute superiority of this method over other aforementioned ones. The method was effectively applied in determining (PPA) in blood and urine samples.

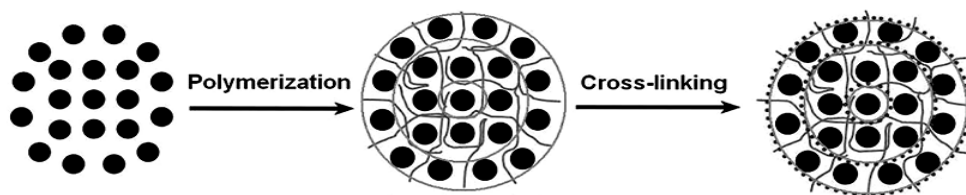


**Fig. 1.** Schematic illustration of the PbS quantum dots sensor functionalized with gelatin synthesis.

## 2. EXPERIMENTAL

### 2-1. Apparatuses

A Shimadzu 1601 PC UV-Vis spectrophotometer with a 1cm cell was used for recording all spectra and absorbance measurements (Shimadzu, Japan) at room temperature. Fluorescence spectra were performed on a Hitachi F-7000 fluorescence spectrometer (Tokyo, Japan). X-ray photoelectron spectroscopy (XPS) measurements were carried out using an ESCALAB 205 X<sub>i</sub> spectrometer (Thermo Fisher Scientific, Waltham, MA, USA). Fourier transform infrared (FT-IR) spectra were recorded on a PerkinElmer (FT-IR spectrum BX, Germany). Time-resolved luminescence intensity decay was recorded on a Horiba JY Fluorolog-3 molecule fluorometer (Paris, France), and samples were excited by a 375 nm laser light source. A Jenway 3510 pH-meter which calibrated against two standard buffer solutions at pH 4.0 and 10.0 was used to measure the pH of the solutions. A Hamilton syringe (10 µl) was used to deliver small volumes of reagent into the cell. The reference cell was contained a membrane without any indicator. All measurements were made in the absorbance mode.

### 2.2. Reagents and materials

All chemicals, lead sulfide (PbS), gelatin, glutaraldehyde, from Merck Company. Phenylpropanolamine (PPA) drug (98.0 %), purchased from India Company. Hydrochloric acid and methanol were purchased from Merck Company, solution (Merck, Darmstadt, Germany).

Universal buffer solutions were prepared from boric acid / acetic acid / phosphoric acid (0.04 M each). The final pH was adjusted by the addition of 0.2M sodium hydroxide. Stock solutions of 10.0 µg L<sup>-1</sup> of interfering drugs. Were prepared by dissolving appropriate amounts of suitable salts in double distilled water.

### 2.3. Pretreatment of real samples Urine samples

A 10 mL portion of a urine sample (or a spiked urine sample) was treated with 10 mL of concentrated HNO<sub>3</sub> (63%) and an HClO<sub>4</sub> (70%) mixture of 2:1 in a 50 mL beaker covered with a watch glass. The content of the beaker was heated on a hot plate (100 °C, 15 min, 150 °C 10 min). The watch glass was removed and the acid evaporated to dryness at 150 °C HClO<sub>4</sub> (3 mL) was added to the resulting white residue and the mixture was heated at 160 °C to dryness. All heating was carried out under a hood while taking the necessary precautions. Five milliliters of 1 M H<sub>2</sub>SO<sub>4</sub> was added, the mixture heated at 150 °C for 1 min, and the volume made up to the mark in a 50 mL volumetric flask. Aliquots (7 mL) of the resulting clear solution were analyzed according to the described procedure [30].

### Blood sample

Homogenized blood sample 20 mL was weighed accurately and in a 200 mL beaker was digested in the presence of an oxidizing agent with addition of 10 mL concentrated HNO<sub>3</sub> and 2 mL HClO<sub>4</sub> 70 % was added and heated for 1 h. The content of beaker was filtered through a Whatman No. 42 filter paper into a 250 mL calibrated flask and its pH was adjusted to desired value and diluted to mark with de-ionized water. In all of real and synthetic sample amount of (PPA) was found by standard addition method [31].

### 2-4. Synthesis of PbS Quantum Dot–Gelatin Nanocomposites Sensor

The nanoparticle PbS was synthesized in reactive solution prepared using lead nitrate (Pb(NO<sub>3</sub>)<sub>2</sub>) and sulfide sodium (Na<sub>2</sub>S) with concentration of (0.1 M and 0.1 M). The Gelatin pellets were used as a base medium and its concentration was set

to (0.1 M). 20 mL of all the above solutions were prepared separately, using distilled water as a solvent and mixed together in a beaker. 2 ml of glutaraldehyde (25%) was added into the solution as a complexing agent, which can easily bind the metal ions. The reactive vessel with solution was immersed into 20 ml acetone maintained at 40°C and pressure of  $10^{-5}$  mbar. A thermometer was placed in the vessel to measure the temperature of the bath solution and also a temperature sensor and dimer with temperature controller were attached to maintain the constant temperature. The solution was stirred well with the help of magnetic stirrer to maintain the homogeneous mixture. The prepared solution was colorless and turned yellowish after (30 min) and suddenly changed into gray color, these indicate the chemical reactions and also confirm the formation of PbS. The reactive solution was continuously stirred for (2 h). The powder was collected and dried in a hot air oven at (57°C) [32].

### 2.5. Procedure Fluorescent Detection measurements

The ensuing steps were followed for a typical fluorescence emission intensity method experiment: first, a 10 ml volumetric flask was picked and 1ml of PPA ( $10.0\mu\text{g L}^{-1}$ ) was added to it. Second, 1ml PbS Quantum Dot–Gelatin Nano composites ( $2.5\times 10^{-2}\text{ mol L}^{-1}$ ) and then 2 ml of glutaraldehyde (25%) were put into the volumetric flask. The reaction time start point was recorded. After (10 sec), the solution was mixed for another 10 sec and then by adding DW (distilled water) it was volumed. The difference between the quantities of the absorption in a wavelength equal to (335 nm) in a time interval equal to (40- 60 sec), was estimated. By adding (PPA) to the solution, it was observed that fluorescence

emission intensity of the acetonitrile solution of PbS quantum dot–gelatin nanocomposites at wavelength of (335 nm) dropped. At the same time, with the help of fluorometric and UV–visible spectrum ( $\Delta I$  b), the apparent spectral evolution including the formation of a well-defined isobestic point at around (335 nm) was estimated. All reaction steps were repeated by increasing the concentration ( $0.2\mu\text{g L}^{-1}$ ) of the (PPA) drug every (10 sec). Moreover, all the steps were repeated for a reaction. In the fluorometric of (PPA) drug ( $\Delta I$  b) and ultimately ( $\Delta I$ )  $I_0$  blank-I sample. There was a sharp change in the fluorescence emission of the sensor in the (335 nm) region, a continuous increase of (PPA) drug at intervals of (10 sec) in solution and changes in the fluorescence emission intensity of the sensor, peak fluorescence emission during (335 nm), with an increase in fluorescence emission intensity, can be seen in (fig. 3A). UV–visible spectrum (AAb). All these steps would be repeated for a reaction without the presence of (PPA) drug (AAb), finally (AA) AAblank-AAsample is calculated. The spectrum changes are due to the addition of (PPA) drug in the range of ( $0.0\mu\text{g L}^{-1}$  at  $1.1\mu\text{g L}^{-1}$ ) and the formation of a complex. As can be seen, the complex ((PPA) drug-sensor) has absorption peaks at a wavelength of 385 nm (Fig. 3B) [33].

## 3. RESULTS AND DISCUSSION

### 3.1. Characterization of PbS Quantum Dot–Gelatin Nanocomposites Synthesis

#### 3.1.1. FTIR analysis

FTIR spectra for PbS Quantum Dot–Gelatin Nanocomposites Synthesis are shown in (Fig. 4). The vibrational frequencies for stretching bonds in PbS molecule cannot be detected by FTIR analysis. This confirms that PbS doesn't show any definite absorption peaks in the range  $400 - 4000\text{ cm}^{-1}$ . The vibration modes located at  $3423\text{ cm}^{-1}$  can be assigned to the

O–H broad absorption mode due to the hydroxyl group in the compound. The absorption band at  $2928\text{ cm}^{-1}$  corresponds to the C–H stretching vibration mode. The broad absorption near  $1300 - 1000\text{ cm}^{-1}$  confirms the presence of the C–O bond. The absorption band at  $1637\text{ cm}^{-1}$  is due to

the O–H bending vibration from the water molecules adsorbed into the surface. There is a furthermore subtle point that no significant difference between the FTIR spectra of PbS quantum dots with gelatin Synthesis nanoparticles is observed [34].

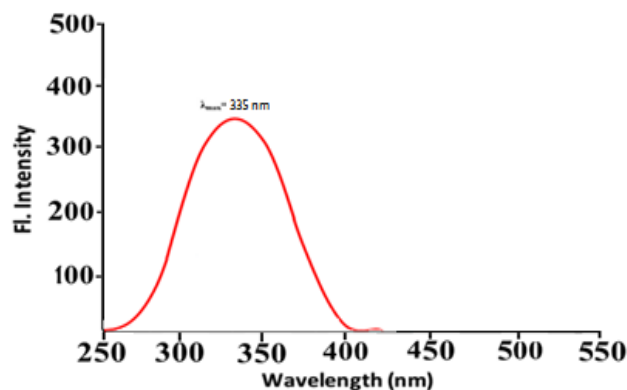


Fig. 2. The Fluorescent Detection of product PbS Quantum Dot–Gelatin Nanocomposites.

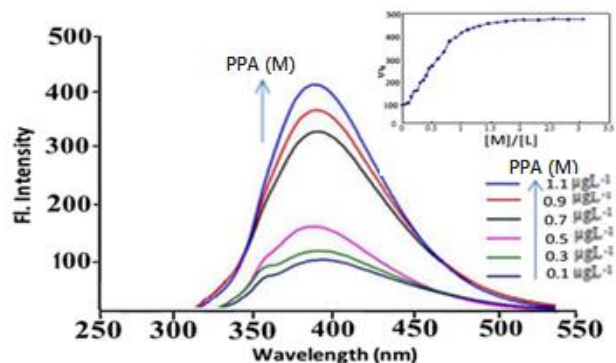


Fig. 3A. The Fluorescent Detection of product PbS quantum dots–gelatin nanocomposites and (PPA) medication (10 sec), and increasing concentration of the (PPA) medication solution ( $0.2\mu\text{g L}^{-1}$ ).

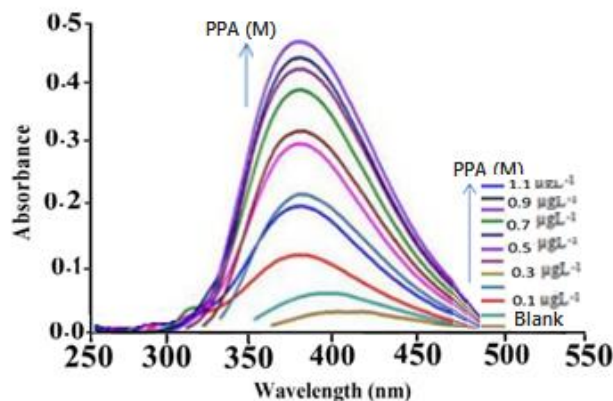


Fig. 3B. The absorption spectra of product PbS quantum dots–gelatin nanocomposites and (PPA) medication (10 sec), and increasing concentration of the (PPA) medication solution ( $0.2\mu\text{g L}^{-1}$ ).

### 3.1.2. XRD analysis

The XRD pattern of the PbS Quantum Dot–Gelatin Nanocomposites is shown in (Fig.5). The synthesized nanopowders are found to be polycrystalline in nature. All detectable peaks corresponding to (111), (420), (331), (400), (222), (311), (220), (200) and (422) planes belong to the pure cubic phase of PbS (JCPDS no. 78–1901) [35].

The graph in (Fig. 6) shows the morphological features and particle size distribution of the PbS Quantum Dot–Gelatin Nanocomposites using SEM micrograph. It has been seen that the particles were mostly spherical with a various size distribution as they form agglomerates. From the particle size distribution, we obtain the average particle size in the range of 37-44 nm very close to those determined by XRD analysis [36].

### 3.1.3. Surface morphology

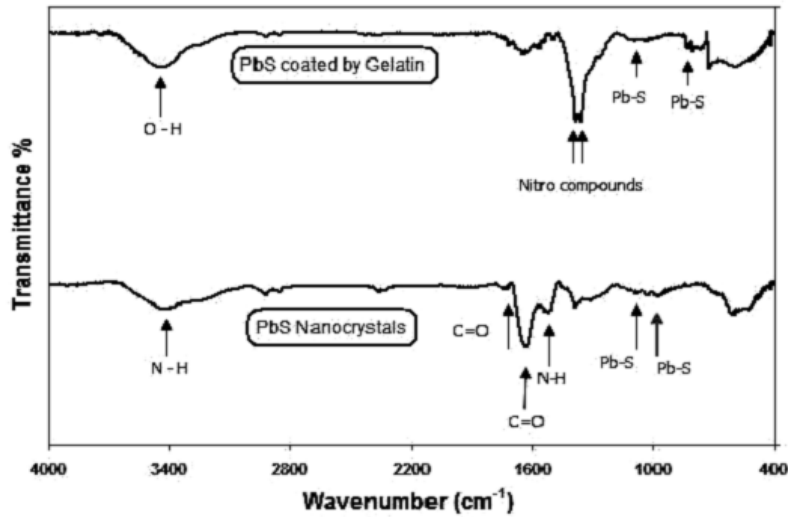


**Fig. 4.** The FT-IR transmittance spectrum of the prepared of synthesized PbS Quantum Dot–Gelatin Nanocomposites.

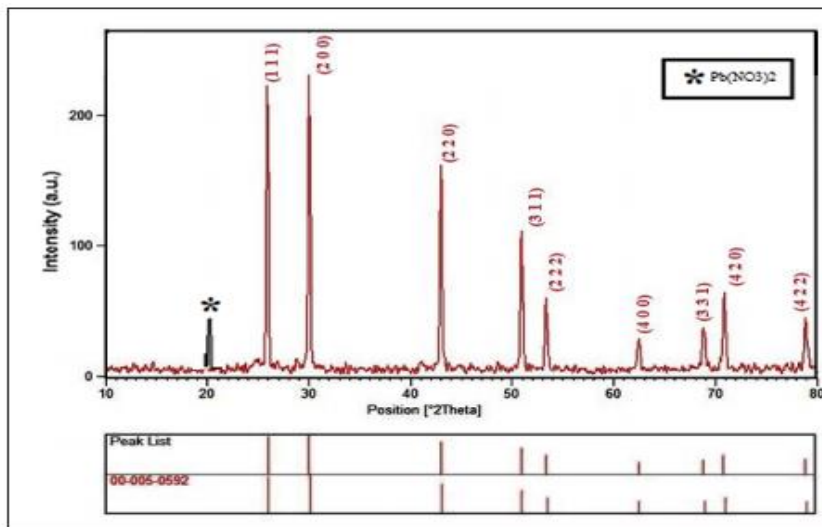


**Fig. 5.** The XRD image of the prepared of synthesized PbS Quantum Dot–Gelatin Nanocomposites.

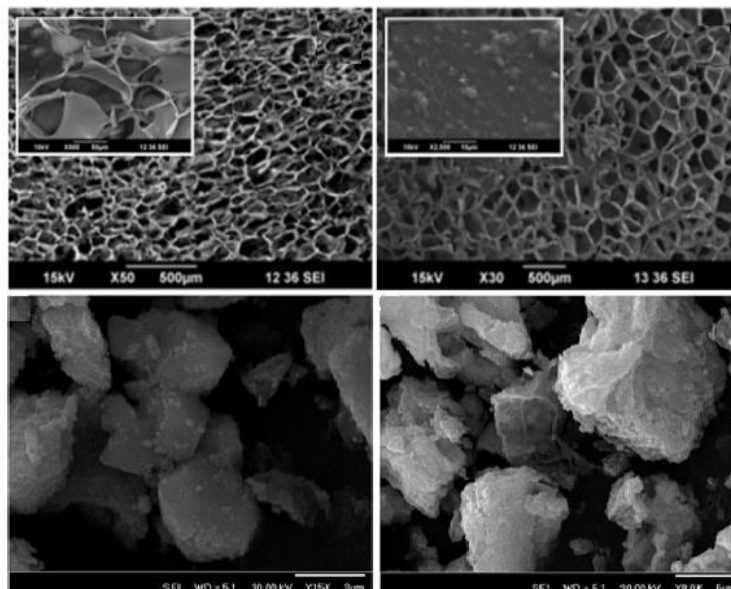


**Fig. 6.** The (SEM) image of synthesized PbS Quantum Dot-Gelatin Nanocomposites.

### 3.2. Optimization of Sensing Conditions

It is interesting that the fluorescence intensity of the as-prepared PbS Quantum Dot-Gelatin Nanocomposites was significantly enhanced in the presence of (PPA) drugs. In order to obtain a highly sensitive response for the detection of (PPA) drugs the optimization of pH values, PbS Quantum Dot-Gelatin Nanocomposites and incubation time was carried out systematically.

The pH value of the reaction solution could greatly influence the interaction between PbS Quantum Dot-Gelatin Nanocomposites and (PPA) drugs. To inspecting The effect of PbS Quantum Dot-Gelatin Nanocomposites, on the reaction rate, 1 ml (PPA) drugs  $10.0 \mu\text{g L}^{-1}$  solution, PbS Quantum Dot-Gelatin Nanocomposites,  $2.0 \times 10^{-2} \text{ mol L}^{-1}$  and 2 ml of glutaraldehyde (25%) are added to the volumetric flask 10 ml and by adding distilled water. fluorescence intensity of solution was measured. The fluctuating pH values in the range of 2–9 of the (PPA) drugs-PbS Quantum Dot-Gelatin Nanocomposites complex at 385 nm were investigated. As displayed in (Figure 7 A), the fluorescence intensity increased

significantly with the increasing solution pH, and reached its maximum when pH reached 4.0. A possible explanation for this is that the pH influences the (PPA) drug speciation in solution [37, 38]. Therefore, pH 4.0 was selected as the optimum pH value for (PPA) drug detection. Meanwhile, To inspecting The effect of PbS Quantum Dot-Gelatin Nanocomposites, on the reaction rate, 1 ml Phenylpropanolamine (PPA) drugs  $10.0 \mu\text{g L}^{-1}$  solution, 2 ml of glutaraldehyde (25%) and 1 ml, PbS Quantum Dot-Gelatin Nanocomposites,  $0.5 \times 10^{-3}$  to  $4.0 \times 10^{-2} \text{ mol L}^{-1}$  are added to the volumetric flask 10 ml and by adding distilled water. fluorescence intensity of solution was measured. The above mentioned operation was repeated for blank solution (the solution without (PPA) drugs). The results are shown in and (Figure 7 B), based on those results  $2.5 \times 10^{-2} \text{ mol L}^{-1}$  was selected as the desired concentration. In addition, the effect of reaction time on the fluorescence intensity was also studied. It can be seen from (Figure 7 C) that the fluorescence intensity increased rapidly, and reached its maximum at around 60 sec, after which it remained relatively stable. Therefore, a

reaction time of 60 sec was chosen in this experiment.

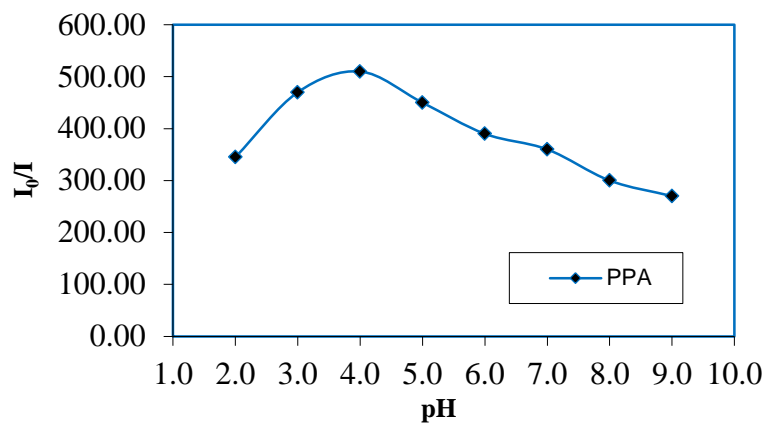


Fig. 7 A. The effect of pH on the rate of reaction.

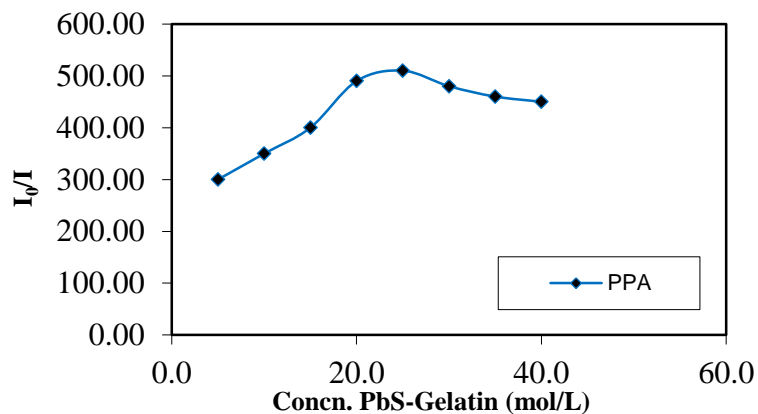


Fig. 7 B. The effect of PbS Quantum Dot-Gelatin Nanocomposites on the reaction rate.

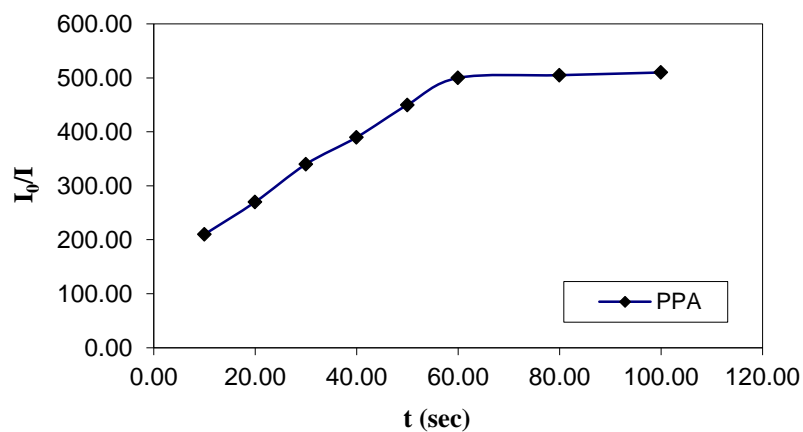


Fig. 7 C. The effect of time on the reaction rate.



### 3.3. Response time

As is known, the response time ( $t_{95\%}$ ) of a sensor, the time required for the response of the sensor towards a certain concentration of the measured ion to reach (95%) of its final value (steady state). Controlling the response time of the membrane is attainable via checking the needed time for the analyte to disperse from the volume of the solution to the PbS Quantum Dot–Gelatin Nano composites interface and to connect with the (PPA) medicament solution. [39]. The response time of the present membrane was tested by recording the fluorescence intensity change at 335 nm from a (pH=4) to a buffered (PPA) drug solution of  $10.0 \mu\text{g L}^{-1}$ . The PbS Quantum Dot–Gelatin Nanocomposites was found to reach 95% of the final signal at 5-120 sec depending on the concentration (Figure 8). In general, the response time is lower in concentrated solutions than dilute solutions.

### 3.4. Calibration graph and reproducibility

These parameters of the The PbS Quantum Dot–Gelatin Nanocomposites was found to

reach 95% of the final signal at 5-120 sec in the determination of (PPA) drug was evaluated by repeatedly exposing the sensing phase membrane to a  $0.05 \mu\text{g L}^{-1}$  (PPA) drug solution and a  $10.0 \mu\text{g L}^{-1}$ . The repeatability was evaluated by performing seven determinations with the same standard solution of (PPA) drug. The relative standard deviation (R.S.D) for the response of The PbS Quantum Dot–Gelatin Nanocomposites was found to reach 95% of the final signal at 60 sec towards a  $10.0 \mu\text{g L}^{-1}$  of (PPA) drug solution was 3.5% ( $n=7$ ).

The reproducibility of the response of different The PbS Quantum Dot–Gelatin Nanocomposites was found to reach 95% of the final signal at 5 -120 sec was also studied. Seven different membranes were prepared from the same batch and they were evaluated by performing the determination of  $10.0 \mu\text{g L}^{-1}$  (PPA) drug. The relative standard deviation for the response of between membranes was a detection limit of  $2.2 \mu\text{g L}^{-1}$  by the fixed-time method of 60 sec in 335 nm [40].

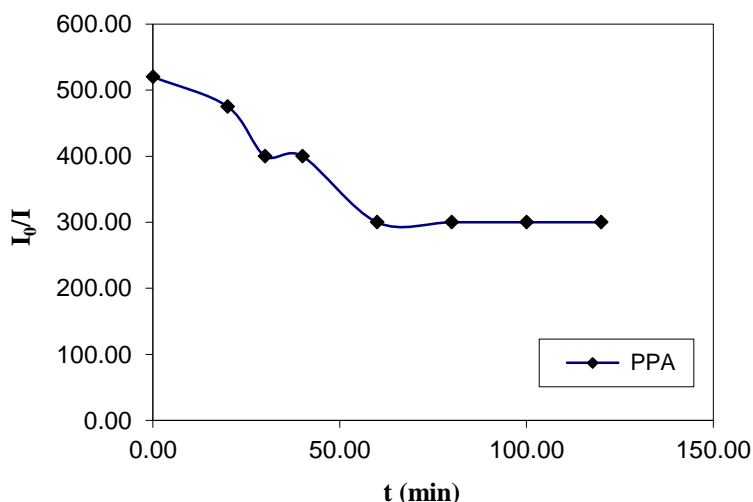


**Fig. 8.** The typical response curve of the PbS Quantum Dot–Gelatin Nanocomposites was found to reach (95%) of the final signal at (50 – 120 sec at 335 nm) as a function of time when the film was exposed to (PPA) drug ( $10.0 \mu\text{g L}^{-1}$ ).

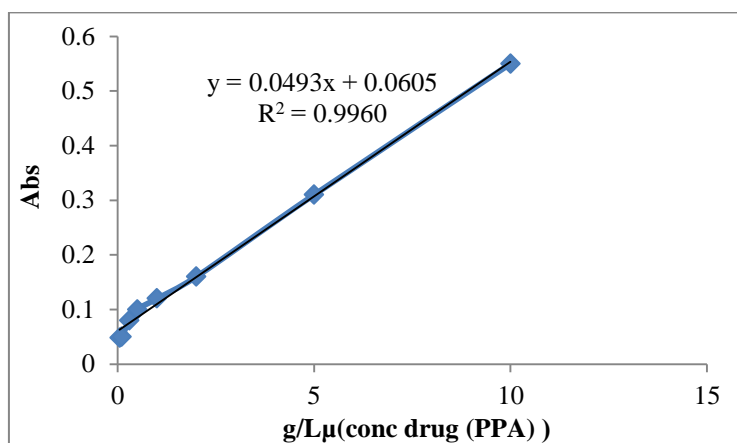


Fig. 9. Calibration graph for (PPA) drug.

### 3.5. Optimum values of parameters

The optimum values of parameters are demonstrated in Table.1. The method can be used as an alternative method for (PPA) medicament measurement owing to advantages like excellent selectivity and sensitivity, low cost, simplicity, low detection limit and no need in utilizing organic harmful solvent.

Table 1. Investigation of method repeatability at conditions

Parameter	Optimum Value for Phenylpropanolamine (PPA) drug
Phenylpropanolamine (PPA) drug ( $\mu\text{g L}^{-1}$ )	(10.0 $\mu\text{g L}^{-1}$ )
PbS quantum dot-gelatin nanocomposites (M)	( $2.5 \times 10^{-2}$ M)
pH	4.0
Equilibration time (sec)	(60.0 sec)
Linear range ( $\text{mol L}^{-1}$ )	0.05 – 10.0 ( $\mu\text{g L}^{-1}$ )
Detection limit ( $\text{mol L}^{-1}$ )	2.2 ( $\mu\text{g L}^{-1}$ )
Accuracy and precision	High
Advantages	High repeatability, sensitivity, selectivity, wide linear range and no need to organic solvent

### 3.6. Interference Studies

After establishing the measurement method, to evaluate the selectivity of the prepared. The PbS quantum dot-gelatin nanocomposites sensor for determining the (PPA) drug the effect of various substances on the determination of (PPA) drug ( $10.0 \mu\text{g L}^{-1}$ ) for method respectively was tested under optimum conditions. Several representative potential interferences such as inorganic cations, anions, molecular species and dyes were investigated individually for their effect on (PPA) drug recovery. Tolerance Limits were defined by the concentration of interferences which caused on <5% error in the determination of (PPA) drug [41,42]. The obtained mean recoveries and standard deviation ranged between 102.0% - 98.0% respectively are shown in (Table 2).

The results showed that most of the other medications studied did not have much effect on the measurement of (PPA) drug and among them, compounds with a more similar structure or with more functional groups are more disturbing, which It may be related to their hydrogen interactions or the molecule of the (PPA) drug and thus reduce the measurement of the (PPA) drug in the analyte sample. As exhibited in (Table.2), the tolerance limit was determined as the max concentration of the interfering substance which resulted

in an error less than ( $\pm 5\%$ ) for determination of (PPA) drug. The So selectivity of the recommended method was proven.

**Table 2.** Effects of the matrix drugs on the recoveries of the examined (PPA) drug (N=6)

Foreign species	Tolerance limit (ng/mL)
Amoxicillin, Ampicilline, Acetaminophene, Cortisone, Cyclosporine	1000
Tramadol, Metadone	750
$\text{NH}_4^+$ , $\text{Mg}^{2+}$ , $\text{F}^-$ , $\text{K}^+$ , $\text{Cu}^{2+}$ , $\text{Fe}^{3+}$ , $\text{Ca}^{2+}$ , $\text{Cl}^-$ , $\text{I}^-$	500
Naratriptan, Rizatriptan, Sumatriptan and Zolmitriptan	100

### 3.7. Real Sample Analysis

To evaluate whether the fluorescent the PbS Quantum Dot–Gelatin Nanocomposites was found to reach 95% of the final signal at 5-120 sec probe is applicable to natural systems; in urine and blood samples were investigated. Analytical results showed that the fluorescence tests were affected in the real samples due to the complex matrix. However, the fluorescence The PbS Quantum Dot–Gelatin Nanocomposites was found to reach 95% of the final signal at 5-120 sec probe exhibited excellent performance [43]. The average recoveries of two spiked samples ranged from 98.0% to 102.0%, with RSDs of 2.8–3.8% (n=3) at three spiked levels (Table 3), which indicated the practicality and reliability of the PbS Quantum Dot–Gelatin Nanocomposites was found to reach 95% of the final signal at 60 sec probe for the detection of (PPA) drug in various samples. Table 3. Analytical results for

(PPA) drug sensing in real samples [44].

## 4. CONCLUSION

Drugs fluorescence assay techniques are highly specific and sensitive, but their use is restricted due to (PPA) drug instability and assay complexity. In this study, ratiometric fluorescent biosensors for (PPA) drug detection were successfully fabricated. The high recovery percentage of two sensing membranes in urine and blood samples highlights their potential application for the determination of (PPA) drug concentrations in clinical chemistry. In addition, the successful development of the ratiometric fluorescent biosensors would be of a great significance in high-throughput screening techniques in analytical biochemistry.

The reaction is followed fluorometrically by measuring the absorbance at 335.0 nm.  $2.5 \times 10^{-2} \text{ mol L}^{-1}$  PbS with gelatin sensor, calibration graph in the range of 0.05 - 10.0  $\mu\text{g L}^{-1}$  (PPA) drug. The absorbance is linear from 0.05 up to 100.0  $\mu\text{g L}^{-1}$  in aqueous solution with repeatability (RSD) of 3.5% at a concentration of 10.0  $\mu\text{g L}^{-1}$  and a detection limit of 2.2  $\mu\text{g L}^{-1}$  by the fixed-time method of 60 sec. The relative standard deviation for 10.0  $\mu\text{g L}^{-1}$  (PPA) drug is %95. The method due advantages such as high selectivity and sensitivity, low detection limit, simplicity, low cost and no need to extraction and using organic harmful solvent with respect to previously reported methods is an alternative method for (PPA) drug determination. Also, it was applied propitiously for measuring (PPA) medicament in urine and blood samples.

**Table 3.** Recovery of trace (PPA) drug from urine and blood sample after application of presented procedure (n=3)

Samples	Added ( $\mu\text{g mL}^{-1}$ )	Founded ( $\mu\text{g mL}^{-1}$ )	RSD %	Recovery %
Urine	0/0	2/94	3/7	----
	0/5	8/03	2/8	102/0
Blood	0/0	14/85	3/8	----
	0/5	19/75	3/0	98/0

## ACKNOWLEDGEMENTS

The authors gratefully acknowledge partial support of this work by the Islamic Azad University, Branch of Omidyeh Iran.

## REFERENCES

- [1] R. Brückner, I. Hackbarth, T. Meinertz, B. Schmelzle, H. Scholz, The positive inotropic effect of phenylephrine in the presence of propranolol. Increase in time to peak force and in relaxation time without increase in c-AMP, *Naunyn-Schmiedeberg's archives of pharmacology*. 303 (1978) 205-211.
- [2] N. A. Flavahan, Phenylpropanolamine constricts mouse and human blood vessels by preferentially activating  $\alpha_2$ -adrenoceptors, *J. Pharmacol. Exp. Ther.* 313 (2005) 432-439.
- [3] British Pharmacopoeia. The stationary office, electronic version, London. 305 (2013) 1227, 1099.
- [4] A. L. Suryan, V. K. Bhusari, K. S. Rasal, S.R. Dhaneshwar, Simultaneous quantitation and validation of paracetamol, phenylpropanolamine hydrochloride and cetirizine hydrochloride by RP-HPLC in bulk drug and formulation, *Int. J. Pharm. Sci. Drug Res.* 3 (2011) 303-308.
- [5] E. E. Balint, G. Falkay, G.A. Balint, Khat-a controversial plant, *Wien, Klin. Wochenschr.* 121 (2009) 604-614.
- [6] S. Azhagvuel, R. Sekar, Method development and validation for the simultaneous determination of cetirizine dihydrochloride, paracetamol, and phenylpropanolamine hydrochloride in tablets by capillary zone electrophoresis, *J. Pharm. Biomed. Anal.* 43 (2007) 873-878
- [7] Z. B. Zhang, Z. G. Shen, J. X. Wang, H. Zhao, J. F. Chen, J. Yun, Nanonization of megestrol acetate by liquid precipitation, *Ind. Eng. Chem. Res.* 48 (2009) 8493-8499.
- [8] A. E. Shal, A. K. Attia, Adsorptive stripping voltammetric behavior and determination of zolmitriptan using differential pulse and square wave voltammetry, *Anal. Bioanal. Electrochem.* 5 (2013) 32-45.
- [9] M. Ghalkhani, S. Shahrokhian, F. G. Bidkorbeh, Voltammetric studies of sumatriptan on the surface of pyrolytic graphite electrode modified with multi-walled carbon nanotubes decorated with silver nanoparticles, *Talanta*. 80 (2009) 31-38.
- [10] S. Karakuş, I. Küçükgüzel, S. G. Küçükgüzel, Development and validation of a rapid RP-HPLC method for the determination of cetirizine or fexofenadine with pseudoephedrine in binary pharmaceutical dosage forms, *J. Pharm. Biomed. Anal.* 46 (2008) 295-302.
- [11] K. Sunil, K. Yogesh, K. Abhijeet, Simultaneous estimation of cetirizine hydrochloride, phenylpropanolamine hydrochloride and paracetamol by RP-HPLC method, *Int. J. Pharm. Life. Sci.* 4 (2013) 3122-3132.
- [12] K. Abbasia, M. I. Bhangera, M. Y. Khuhawar, Capillary gas chromatographic determination of phenylpropanolamine in pharmaceutical preparation, *J. Pharm. Biomed. Anal.* 41 (2006) 998-1001.
- [13] S. N. Makhija, P. R. Vavia, Stability indicating HPTLC method for the simultaneous determination of pseudoephedrine and cetirizine in pharmaceutical formulations, *J. Pharm. Biomed. Anal.* 25 (2001) 663-667.
- [14] A. Dalpiaz, N. Marchetti, A. Cavazzini, L. Pasti, S. Velaga, E. Gavini, S. Beggiato, L. Ferraro, Quantitative determination of zolmitriptan in rat blood and cerebrospinal fluid by reversed phase HPLC-ESI-MS/MS analysis: application to in vivo preclinical pharmacokinetic study, *J. Chromatogr. B* 901 (2012) 72-78.
- [15] S. B. Wankhede, K. A. Lad, S. S. Chitlange, Development and validation of UV-spectrophotometric methods for simultaneous estimation of cetirizine

- hydrochloride and phenylephrine hydrochloride in tablets, *Int. J. Pharm. Sci. Drug. Res.* 4 (2012) 222–226.
- [16] M. I. Walash, N. El-Enany, S. Saad, A new spectrophotometric method for determination of phenylpropanolamine HCl in its pharmaceutical formulations via reaction with 2,3,5,6-tetrachloro-1,4-benzoquinone, *Int. J. Biomed. Sci.* 6 (2010) 150–157.
- [17] P. Vinas, C. Lopez-Erroz, F. J. Cerdan, Hernandez-Cordoba, Determination of phenylpropanolamine and methoxamine using flow-injection with fluorimetric detection, *Talanta*. 47 (1998) 455–462.
- [18] F. Shahrouei, S. Elhami, E. Tahanpesar, highly Sensitive detection of Ceftriaxone in water, Food, Pharmaceutical and biological samples based on gold nanoparticles in aqueous and micellar media. *J. Spectrochim Acta A Mol Biomols Spectrosc.* 203 (2018) 287.
- [19] N. D. Tan, J. H. Yin, G. Pu, Y. Yuan, L. Meng, N. Xu, A simple polyethylenimine-salicylaldehyde fluorescence probe: Sensitive and selective detection of  $Zn^{2+}$  and  $Cd^{2+}$  in aqueous solution by adding  $S^{2-}$  ion, *J. Chem. Phys. Lett.* 666 (2016) 68–72.
- [20] Y. Dai, K. Yao, J. Fu, K. Xue, L. Yang, K. Xu, A novel 2-(hydroxymethyl)quinolin-8-ol-based selective and sensitive fluorescence probe for  $Cd^{2+}$  ion in water and living cells, *Sens. Actuators. B.* 251 (2017) 877–884.
- [21] W. B. Huang, W. Gu, H. X. Huang, J.B. Wang, W.X. Shen, Y.Y. Lv, J. Shen, A porphyrin-based fluorescent probe for optical detection of toxic  $Cd^{2+}$  ion in aqueous solution and living cells, *Dyes. Pigments.* 143 (2017) 427 – 435.
- [22] N. B. Brahim, N. B. H. Mohamed, M. Echabaane, M. Haouari, R.B. Chaabane, M. Negreie, H.B. Ouada, Thioglycerol-functionalized CdSe quantum dots detecting cadmium ions, *Sens. Actuators. B.* 220 (2015) 1346 – 1353.
- [23] L. Shang, S. Dong, G.N. Nienhaus, Ultra-small fluorescent metal nanoclusters: Synthesis and biological applications. *Nano Today.* 6 (2011) 401–418.
- [24] H. Xu, K.S. Suslick, Water-soluble fluorescent silver nanoclusters, *Adv. Mater.* 22 (2010) 1078–1082.
- [25] Y. Lu, W. Chen, Sub-nanometre sized metal clusters: From synthetic challenges to the unique property discoveries, *J. Chem. Soc. Rev.* 41 (2012) 3594–3623.
- [26] V. Venkatesh, A. Shukla, S. Sivakumar, S. Verma, Purine-stabilized green fluorescent gold nanoclusters for cell nuclei imaging applications, *ACS. Appl. Mater. Int.* 6 (2014) 2185–2191.
- [27] C. Knoblauch, M. Griep, C. Friedrich, Recent advances in the field of bionanotechnology: An insight into optoelectric bacteriorhodopsin, quantum dots, and noble metal nanoclusters, *Sensors.* 14 (2014) 19731–19766.
- [28] Y. Yang, H. Wang, K. Su, Y. Long, Z. Peng, N. Li, F. Liu, A facile and sensitive fluorescent sensor using electrospun nanofibrous film for nitroaromatic explosive detection, *J. Mater. Chem.* 21 (2011) 11895–11900.
- [29] W. C. Chan, S. Nie, Quantum dot bioconjugates for ultrasensitive nonisotopic detection, *Science.* 281 (1998) 2016 – 2018.
- [30] A. Shokrollahi, H.E. Haghghi, E. Niknam, and K. Niknam, Application of cloud point preconcentration and flame atomic absorption spectrometry for the determination of cadmium and zinc ions in urine, blood serum and water samples, *Quim. Nova. Sao. Paul.* 36 (2013) 273-282.
- [31] N. Zeighami, S. Bagheri, N. Shadmani, Application of Flotation and Spectrophotometric Detection for Preconcentration and Separation of Trace Amounts of Cadmium Ion Using a New Ligand 3-((1H indole-3-yl) (4-Cyano Phenyl) Methyl) 1H Indole (ICPMI) in Real Samples. *Hacettepe. J. Biol. Chem.* 45 (2017) 277.
- [32] N. Nadji, L. Nouri, A. Boudjemaa, D. Messadi, Predicting retention indices of PAHs in reversed-phase liquid

- chromatography: A quantitative structure retention relationship approach. *J. Serbian Chem. Soc.* 85 (2020) 1-8.
- [33] J. S. Justin Packia Jacob, F. A. Narayanan, Synthesis of silver nanoparticles using Piper longum leaf extracts and its cytotoxic activity against Hep-2 cell line *Colloids and Surfaces B: Biointerfaces.* 91 (2012) 212–214.
- [34] M. Koneswaran, R. Narayanaswamy, CdS/ZnS core-shell quantum dots capped with mercaptoacetic acid as fluorescent probes for Hg(II) ions, *Microchimica Acta.* 178 (2012) 171-178.
- [35] Y. Zhao, J. Zou, W. Shi, In situ synthesis and characterization of lead sulfide nanocrystallites in the modified hyperbranched polyester by gamma-ray irradiation, *Mater. Sci. Eng.* 121 (2005) 20-24.
- [36] S. Baluta, A. Swist, J. Cabaj, K. Malecha, Point-of-Care Testing – Biosensor for Norepinephrine Determination. *Int. J. Electronics. Telecom.* 66 (2020) 369-372.
- [37] T. S. Shyju, S. Anandhi, R. Sivakumar, R. Gopalakrishnan, Studies on Lead Sulfide (PbS) Semiconducting Thin Films Deposited from Nanoparticles and Its NLO Application, *Int. J. Nanoscience.* 13 (2014) 1450001-1450012.
- [38] C. Krishnaraj, E. G. Jagan, S. Jagan, P. Rajasekar, P. T. Selvakumar, N. Kalaichelvan, Synthesis of silver nanoparticles using *Acalypha indica* leaf extracts and its antibacterial activity against water borne pathogens, *Colloids and Surfaces. B: Biointerfaces.* 76 (2010) 50–56.
- [39] M. Pargari, F. Marahel, B. Mombini Godajdar. Design and Evaluation and Synthesis a Starch-Capped Silver Nanoparticles Sensor and Determination trace Sulfacetamide Drug in the Presence Sodium borohydride in Blood and Urine Samples with Kinetic Spectrophotometric Method. *J. Phys. Theor. Chem.* 17 (2020) 1-14.
- [40] E. Keskin, S. Allahverdiyeva, E. Şeyho, Y. Yardim, Determination of tramadol in pharmaceutical forms and urine samples using a boron-doped diamond electrode. *J. Serb. Chem. Soc.* 84
- [41] S.S. Liang, L. Qi, R.L. Zhang, M. Jin, Z.Q. Zhang, Ratiometric fluorescence biosensor based on CdTe quantum and carbon dots for double strand DNA detection, *Sens. Actuators. B.* 244 (2017) 585–590.
- [42] P. Dutta, D. Saikia, N. C. Adhikary, N.S. Sarma, Macromolecular Systems with MSA-Capped CdTe and CdTe/ZnS Core/Shell Quantum Dots as Superselective and Ultrasensitive Optical Sensors for Picric Acid Explosive, *ACS. Appl. Mater. Interfaces.* 7 (2015) 24778 – 24789.
- [43] K. N. Prashanth, K. Basavaiah, M. S. Raghu, Spectrophotometric determination of zolmitriptan in bulk drug and pharmaceuticals using vanillin as a reagent, *ISRN. Anal. Chem.* (2013) 1–7.
- [44] H. Xie, F. Zeng, S. Wu, Ratiometric fluorescent biosensor for hyaluronidase with hyaluronan as both nanoparticle scaffold and substrate for enzymatic reaction, *Biomacromolecules.* 15 (2014) 3383–3389.
- [45] S. Baluta, K. Malecha, A. Swist, J. Cabaj, Fluorescence Sensing Platforms for Epinephrine Detection Based on Low Temperature Cofired Ceramics. *Sensors.* 20 (2020) 1429.